Modeling rf breakdown arcs II: plasma/materials interactions

Z. Insepov, J. Norem, Th. Proslier*
Argonne National Laboratory, Argonne, IL 60439 USA

S. Mahalingam, S. Veitzer
Tech-X Corp., Boulder, CO, 80303 USA
(Dated: April 19, 2022)

Continuing the description of rf vacuum arcs from an earlier paper, we describe some aspects of the interaction of vacuum arcs that involve the surface. This paper describes aspects of plasma materials interactions that affect the arc and models measurement of the surface field using the Tonks-Frenkel and the spinodal electrohydrodynamic instabilities, a realistic model for the generation and evaluation of high field enhancements, unipolar arcs, electromigration and some aspects of the dependence on the static magnetic field.

PACS numbers: 29.20.-c, 52.80.Vp

I. INTRODUCTION

We have primarily discussed the plasma parameters and plasma evolution in Part I of this paper [1]. In part II we describe plasma/materials interaction mechanisms that control the development of the plasma. The surface conditions described in Part I are determined fairly precisely, however in many cases the relevant data is not available, or not provided with useful precision, requiring a specific modeling effort. We describe simulations of self sputtering from surfaces at high temperatures and high electric fields, measurements of the surface fields using surface morphology, simulating high field enhancements from realistic surface morphologies, possible unipolar arc mechanisms as transient phenomena and the effects of fatigue, creep, field evaporation and electromigration on materials subjected to high electric fields. In this paper we can consider only results immediately relevant to arcing mechanisms, with some relevant references, since the literature is extensive.

II. SELF SPUTTERING

This discussion summarizes results of a recent paper modeling the effects of high fields and liquid surfaces with Molecular Dynamics. As shown in a number of papers, [2, 3], the development of a self-sustaining arc depends on the self-sputtering coefficient being significantly larger than 1. We have explored the self-sputtering coefficient for copper ions as a function of surface temperature at or above the melting point and for high electric surface fields using molecular dynamics calculations showing that both high surface temperatures and high surface electric fields can independently increase the self sputtering rate to greater than 10 either near the melting point of the material or at fields at or above 3 GV/m; see Figs. 11 and 12 of Ref. [2]. The dynamics of sputtering from liquid metals or sputtering from surfaces at high electrical gradients has not been extensively expored, so modeling these effects seems to be the most useful way to evaluate the effects. Melting decreases the binding energy of atoms at the surface and high electric field gradients induces surface charge that should pull atoms from the surface. It seems reasonable to expect that the combination of both high fields and high temperatures would further increase the self-sputtering. High self-sputtering rates produce fluxes of neutrals into the plasma that must either increase the plasma density or produce increased fluxes of ions that impact the surface, both processes ultimately increasing the plasma density and thus surface field.

We assume that the primary damage mechanism is erosion due to self-sputtering, with an erosion rate, in meters/sec, that is effectively determined by the thermal current times the sputtering yield,

$$r \sim n_I \; v_t \; Y(\phi, \lambda_D, T)/V_{Cu},$$

where n_I is the density of plasma ions, v_t is their thermal velocity $Y(\phi, \lambda_d, T)$ is their self-sputtering yield for a given plasma potential, Debye length and surface temperature, and V_{Cu} is the volume of a copper atom. The thermal velocity is expressed as.

$$v_t = \sqrt{kT_e/M},$$

and depends only on the electron temperature, T_e, and the ion mass M. The intensity of these currents is described in Ref [4]. For the parameters we describe in this paper ($T_I \sim 1$ eV. $n_I \sim 10^{24}$ m^{-3}, these erosion rates are on the order of 1 m/s. For rf pulse length on the order of 25 μs, this would give craters with a depth on the order of 25 μm. In combination with the high surface temperature described by the plasma code (see Ref I), we find we are describing an environment where the metallic surface cannot survive. The damage (primarily craters) seen on cavity surfaces is consistent with the high erosion rates described here. We are preparing models that can more fully describe the surface damage produced.

*Electronic address: norem@anl.gov

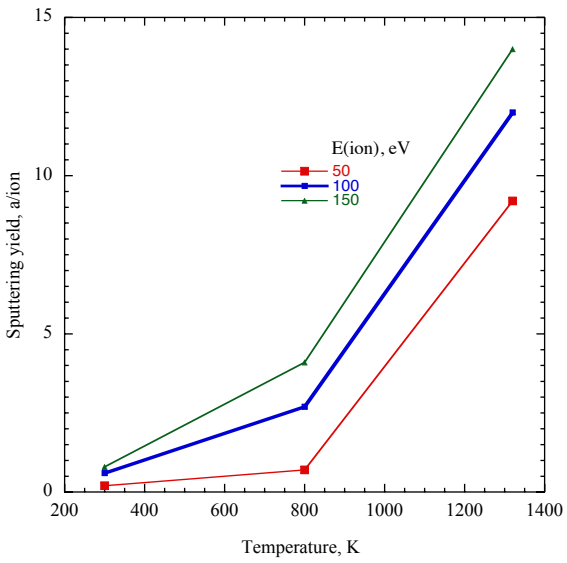

FIG. 1: Calculated sputtering yield as a function of T, showing the large increase at the melting point. [2]

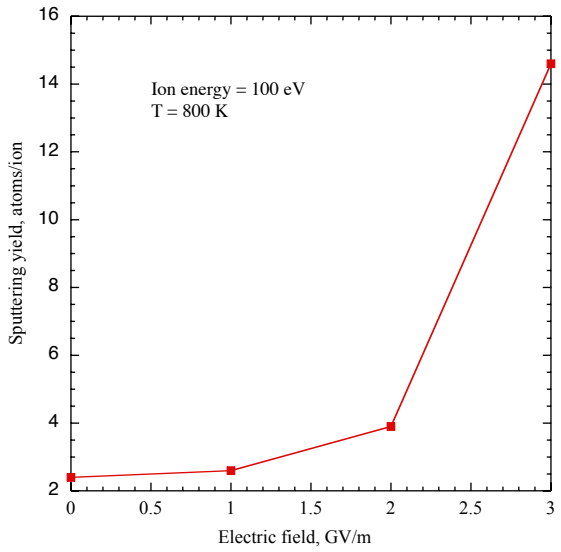

FIG. 2: Calculated sputtering yield as a function of E from molecular dynamics showing a large increase as the electric field increases. [2]

III. MEASURING THE SURFACE ELECTRIC FIELD FROM SURFACE MORPHOLOGY

One of the fundamental problems in the study of arcs is precise measurements of the basic plasma parameters. In the model described here, the surface field is perhaps the most important parameter because it drives the field emission currents and the ion currents. Because these arcs occur unpredictably over large areas, last only a few ns, have sizes of a few μm, and the surface fields are very effectively screened a few ns into the plasma, direct measurements of the surface field seems difficult. Here we describe an indirect method of measuring the surface electric field by looking at the surface damage left by the arc.

Formation of surface periodic and irregular structures such as ripples, cones, and/or bubbles or combination of them were observed on rf cavity surfaces encountered vacuum breakdown , on the first walls on the Tokamak chamber , on the surfaces irradiated by laser beams, during hypervelocity impact welding, and are subjects of detailed studies of experiments and computer simulations. Therefore, understanding of the ripple and microstructure formation is important for all these research fields and can be used, we believe, to estimate the range of surface fields at the center of an active arc..

There are at least two different types of surface ripples. The first type is formed on an ion bombarded and heavily eroded surface, either conducting or insulating. The crests of such type of ripples are oriented perpendicular to the direction of incoming ion beam, so that the wave vectors of the 2-d surface wave structure in oriented parallel to the ion beam. The direction of the ion beam should be inclined to the surface, to be able to create ripples since normally oriented beams do not create ripples. These effects are described by the Bradley-Harper model [5, 6]. Impact of clusters has also been seen to produce surface ripples in Gas Cluster Ion Beams (GCIB) [7]. Ripples have also been seen in surfaces exposed to high powered lasers, and there is an extensive literature on this subject.

The second type of ripples are similar to capillary waves on a liquid surface and can be created on a conductive surface in a strong surface electric field. The appearance and dynamics of capillary waves under a wide range of conditions is a well-understood phenomenon [8]. These structures can be driven by a number of perturbations and there is a very extensive literature on the subject. This field is primarily based by work done by Tonks and Frenkel in the 1930s, where the basic dynamics and stability were worked out [9, 10]. Our interest in this phenomenon is related to the possibility that these structures can be used to help describe the environment in the interior of dense plasma arcs. We argue that surface structure seen in Scanning Electron Microscope (SEM) photographs of arc damage can be used to constrain the average surface electric field in the arc, since the capillary wave dimensions are a function of the electric field, modified by the plasma pressure. Our measurements imply these electric fields are very large, on the order of 1 GV/m, very near the field at which the whole surface could be subject to field emission. Any measurement of the surface electric field at the interior of an arc must contend with the fact that the plasma neutralizes this electric field close to the surface so the electric field may exist over dimensions of a few nm, the field may exist for only a few ns, and the plasma above the surface may be a highly dense, non-Debye plasma, which itself is not

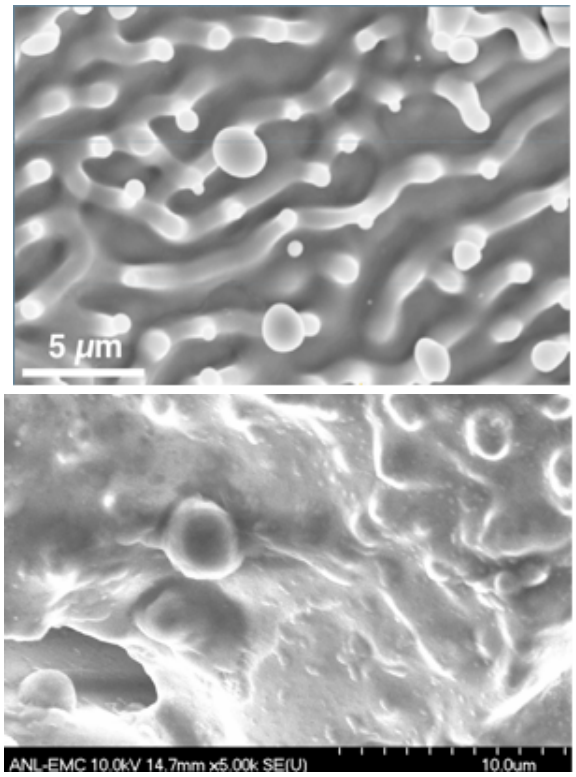

FIG. 3: SEM images showing microstructure on the surface of heavily damaged rf structures. a CLIC structure is shown in a) and a Fermilab structure is shown in b). In both cases much of the structures have an approximate scale of 2 μm. The structures shown in b0 are more typical of what is seen in arc pits. The CERN data is shown by permission [13].

well understood and the structure will be affected by a number of other effects as the surface cools down. It is possible that the surface microstructures we see may be artifacts of the structures that were present in the hot plasma, after these structures and the plasma had cooled.

Our approach is to look at capillary waves and microstructure present in the arc pits left over after the arc is gone. The properties of electrostatically driven capillary waves appropriate to our example have been described by He et. al. [11, 12] for different metals, by means of dispersion relations giving the wavelengths and growth times of the waves structures produced.

Other perturbations, in particular ion beam fluxes that are not perpendicular to the surface, can also produce surface structures, however ion impacts seem to be a second order effect since we assume that the ion fluxes would be driven by the sheath potential and must, by definition, be perpendicular to the surface.

We develop both a simplified and more dynamic approach to this problem to evaluate the contributions of a number of different effects, and in this paper we are primarily concerned with first order causes and effects.

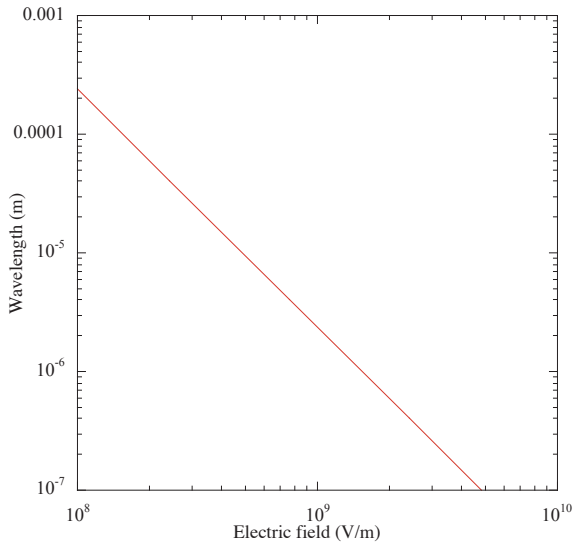

FIG. 4: A plot of the relation between the electrostatic field and "bubble" radius, assuming that the radii of hemispherical structures is determined only by the electrostatic (outward) pressure and the surface tension (inward) pressure on the surface.

A. Experimental studies of structures on liquid metal surfaces

Ripples and structures in liquid metal surfaces are an example of electro-hydrodynamic spinodal decomposition of a flat liquid thin films into structures and cusps (spinodals) that can be either two or three-dimensional. The well known phenomenon of Taylor cones is one example of these structures.

The simplest method of understanding structures on the surface of liquid metals is to consider only the electrostatic tensile stress

$$\sigma = \epsilon_0 E^2/2,$$

where σ, ϵ_0 and E are the surface stress in N/m2, the permittivity of free space, and the electric field and the surface tension, γ, which for molten copper is approximately 1.3 N/m. Equating the pressure due to surface tension and electrostatic forces, as is done to determine the dimensions of bubbles, we find that the equilibrium radius for spherical surfaces is,

$$r = 2\gamma/(\epsilon_0 E^2).$$

or,

$$E = \sqrt{2\gamma/\epsilon_0 r}.$$

This analysis neglects the pressure exerted by plasma ions, so the electric field determined in this way would be a lower limit.

The more general approach is to use the Tonks-Frenkel expression,

$$\omega^2 = \frac{k}{\rho}(\gamma k^2 + \rho g - \frac{E^2}{4\pi}k),$$

where the critical field is defined using the expression,

$$E_{cr} = (64\pi^2\gamma\rho g)^{1/4}.$$

The first paper by Tonks essentially considers the problem of electrostatically driven effects. In the examples we consider here, the electrostatic forces are orders of magnitude larger than the forces due to gravitational acceleration so this term is always neglected. In the case of plasma arcs, the problem is complicated by the contribution of the plasma pressure due to ion fluxes that push on the surface, opposite to the electric tensile stress, so we expect that this analysis would give a lower bound to the expected electric field since it is difficult to evaluate the plasma pressure, which may vary quite widely from example to example. Both the electrostatic and plasma pressure would be expected to be a function of the surface geometry to some extent, further complicating precise solutions.

Pictures of the surfaces of copper structures that have seen significant arcing show a variety of morphologies in arc pits and larger areas, however many surfaces show considerable structure with characteristic dimensions around 2 microns as shown in Figure 3. These figures are examples of the variety of structure seen, and are not necessarily typical, cracks, cones and clusters of small craters are also seen, in addition to particulates, spherical balls and a wide variety of large craters. Study of the morphology of surface damage is complicated by the wide range of operating conditions (stored energy, rf/DC, pulse length, material, surface treatment, lifetime of test, etc.), so it is difficult to make systematic comparisons.

IV. FIELD ENHANCEMENTS

IA number of papers measuring the properties of the pre-breakdown asperities have implied that breakdown is triggered by high surface fields on asperities, but the shape of these asperities has been debated. Defining a field enhancement, $\beta =$ (local field/average surface field), there is considerable data showing field enhancements in the range of 100 1000 [14, 15]. The areas of the pre-breakdown asperities have also been measured, though with less precision, giving dimensions over a wide range, down to a few nm^2.

n the early 1950s Dyke et. al. carefully studied field emission and breakdown with tungsten needles and argued that surface failure was caused by Ohmic heating of the surface due to Fowler-Nordheim field emission however breakdown occurred at the same values of the local surface field, 7 to 10×10^9 V/m [16]. The problem of how local surface fields could be so much larger than the average surface fields on electrode surfaces has not been persuasively explained. Calculations by Rohrbach showed how simple cylindrical geometries could produce large field enhancements [17]. The primary reference seems to be a report that describes the field enhancements produced by a variety of simple geometrical shapes, finding that the fields at the tips of cylinders perpendicular to the surface oriented perpendicular to the surface is enhanced by a factor roughly given by the length of the cylinder divided by its diameter . Although cylindrical structures (whiskers, telephone poles, etc.) seem to be the most common explanation for field enhancements, structures fitting this description, with aspect ratios as large as 1000, are not seen, causing some confusion.

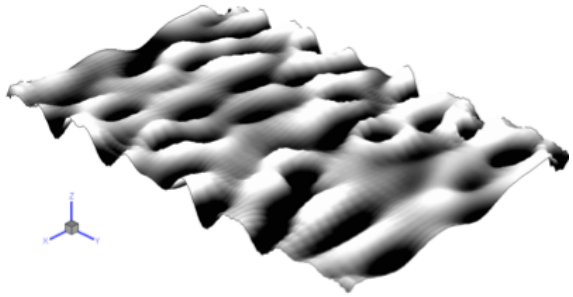

FIG. 5: This figure shows the result of simulation of the Tonks-Frenkel instability based on a numerical solution of the surface dynamics Kuramoto-Sivashinski equation for a copper surface where the surface tension was modified according to Tonks model by adding the negative electric field pressure $-\epsilon_0 E^2/2$ to the effective surface tension.

In the superconducting rf community, where field emission is a critical failure mechanism, it has been assumed that particulates were the primary source of field emission, and examples of the tip-on-tip model seem to explain both what is experimentally seen, and the geometry of the emitters [15, 18].

In addition to the 2 micron structure described above, we experimentally see a variety of sharp edges, corners and cracks in the surface. This paper considers the field enhancements that would be present in these edges, corners and crack systems and how they might function as field emitters. We describe numerical calculations of realistic geometries that produce high enhancement factors and are consistent with experimental data. We find that a variety of structures can produce the expected values of enhancement factors, although with small surface areas, so that a number of sources must contribute. We argue that such structures include sub-micron size cracks, nanoscale tips, sharp cones and periodic wave structures ripples that can be formed on the surfaces of liquid metal, foreign atoms, clusters and clumps placed on the cavity surface with a high electric field. To achieve this goal,

the electrostatic Laplace equations for surface structures were numerically solved by using a finite-element multiphysics simulation package COMSOL [19].

A. Evaluating field enhancements using COMSOL

The COMSOL finite element multiphysics simulation tool is convenient for electromagnetic simulations in 2- and 3-dimensions [1]. It solves the Laplace or Poisson equations for arbitrary geometry by the adaptive finite-element constructions where the smallest element size can be chosen to be at an atomic scale yet the system can be solved within a short computational time. A mesh is a partition of the geometric volume into small units of simple shape in the simulated system. Maxwell equations dont take into account atomistic nature of the charges on the metal surfaces. Therefore, the mesh size was restricted by setting the minimum size to 1 at the sharpest geometric locations.

We used an adaptive mesh structure with the minimal size fixed at 1 Angstrom This condition if not critical and the calculations were performed at different element sizes and the results were obtained at the level where the dependence of the results on the cell size was negligible. The boundary conditions for the solution of the electrostatic problem were chosen as are shown in eq. (1). The ground electrode potential was fixed at 0 V, and the top electrode potential was chosen 10 V, so the average electric field between the electrodes was of 1 V/m.

The electric potential of the top electrode and the total distance between the electrodes H were chosen to generate the electric field 1 V/m everywhere in the system, except near the tips sharp spherical end: The voltage at the top electrode is 2 μV, at at distance of 2 μm; producing field enhancement directly from the plot shown in Fig. 6c : the maximum number on the plot corresponds to the maximum field enhancement.

Insulating boundary conditions for the side surfaces were applied in 2- and 3-dimensional symmetries. Our simulations show close agreement of field enhancement coefficient generated by a sharp cylindrical tip on the Copper surface with the theory, for small aspect ratios. The discrepancies between simulation and theory seen in Fig. 1 for the ratio h/? =100, have no principal origin, since these assessment simulations were performed with lower accuracy to reduce the computational load.

Experimentally, high magnification SEM pictures of arc pits show cracks and pits with a variety of sharp edges at the limit of the resolution of the microscope. Mueller has also shown SEM pictures of a variety of physical shapes that produce high enhancement factors [20, 21]. We assume that these sharp edges contribute to the field enhancements and thus the field emission, and calculate their properties.

Conical asperities are a useful starting point. The enhancements calculated for conical and sharp edged geometries are dependent on how the singularity at the tip is handled. We have compared sharp and rounded geometries and found that the rounded geometry essentially truncates the enhancement at a value comparable to the where the cone radius is equal to the radius assumed for the tip. We are also interested in the tips produced at triple crack junctions, since these seem to be

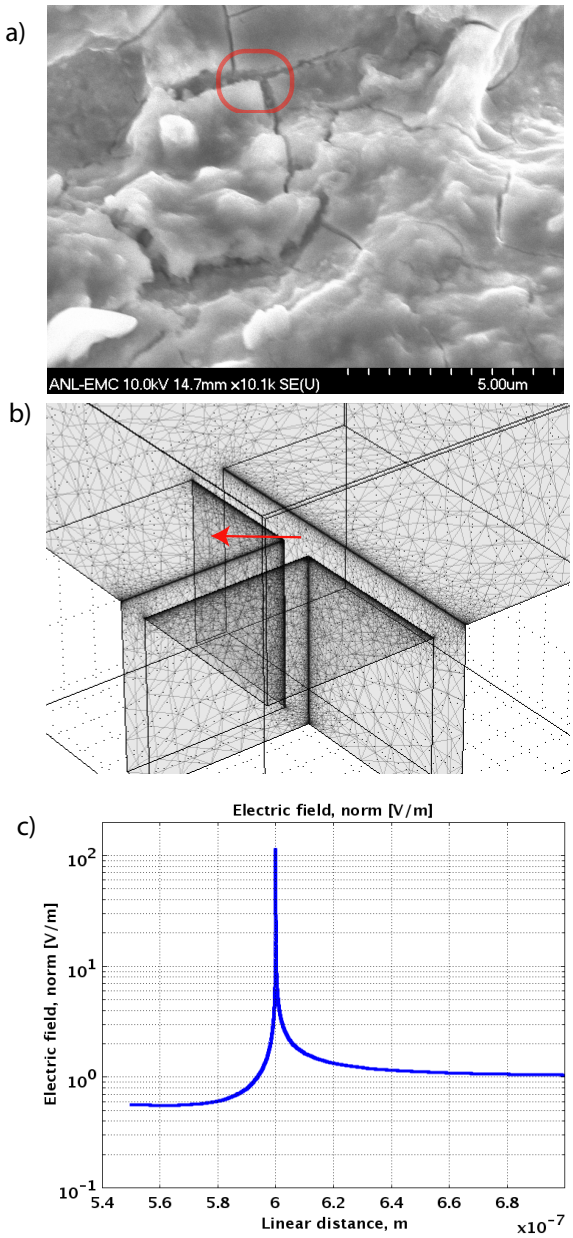

FIG. 6: a) an SEM image of arc pit cracks on the breakdown surface from an rf cavity after a breakdown event showing considerable microstructure. The magnification on plot b) shows our Comsol simulation setting for a triple crack junction and c) shows the calculated field enhancement at the =triple crack junction, with $\beta = 140$, which is close to experimental values in the range of $\sim$ 180 - 200 obtained in cavity measurements.

very numerous in SEM images. While the emission from one of these tips would have insufficient area to produce the observed field emission currents, adding the contributions of many of these tips could produce the few nm^2 produced by fits to the the field emission currents. As seen in the SEM photo, the surface in which these crack junctions is imbedded is not flat, and would be subject to a tip-on-tip enhancement, which could be significantly larger than the simple factor calculated for a flat surface.

We show in Fig. 6 a) SEM photograph at high magnification of the bottom of an arc pit (about 200 microns in diameter) from an rf cavity breakdown event showing numerous cracks running in all directions. Because the crack junctions are numerous and topologically similar to the conical example discussed above, we have modeled the electrostatic fields assuming the tips of these junctions could be sharp.

The numerous cracks in this example can be explained due to rapid thermal cooling of the surface after an arc. The melting point of copper is 1357 deg C, thus molten metal in arc pits must cool about 1000 deg C before it reaches room temperature. If we assume that arcs heat only the top micron of the material, the copper should contract by an amount

$$dL/L = \alpha \Delta T = (17 \times 10^{-6} \times 1000) = 0.017,$$

thus roughly 2% in any linear direction in the hot center of an arc pit should be a crack. The appearance of cracking seems to be a function of rapid heating and cooling of the surface layer. In our samples we see cracks of width about 0.2 microns about 10 microns apart. We expect these crack junctions would produce large numbers of atomically sharp emitters.

We assume that all surface structures with high enhancement factors can be either field emitters or breakdown triggers and are relevant to this paper. The following surface intrusions were simulated: sharp cones with the heights of 100-1000 nm, various types of narrow 2- and 3 dimensional trenches and bars (Fig. 3), the cracks with and without a metal spherical particle above the triple junction of the crack.

V. UNIPOLAR ARCS

Unipolar arcs were first described by Robson and Thonemann, but more recently in the context of laser ablation and tokamak limiters, by F. Schwirzke. A unipolar arc is a plasma in contact with a large metallic surface [22, 23]. These arcs can be produced in a large number of ways,. A recent workshop at Argonne has summarized many aspects of the theory and applications of unipolar arcs. We find that the best reference on this mechanism is [23, 24], however we are considering the option that the unipolar arc could be a transient [25].

OOPIC simulations in Ref [1] have shown that as the ion density increases, the excess net charge density,

$$n_n = (n_i - n_e) \sim 10^{20}/m^3,$$

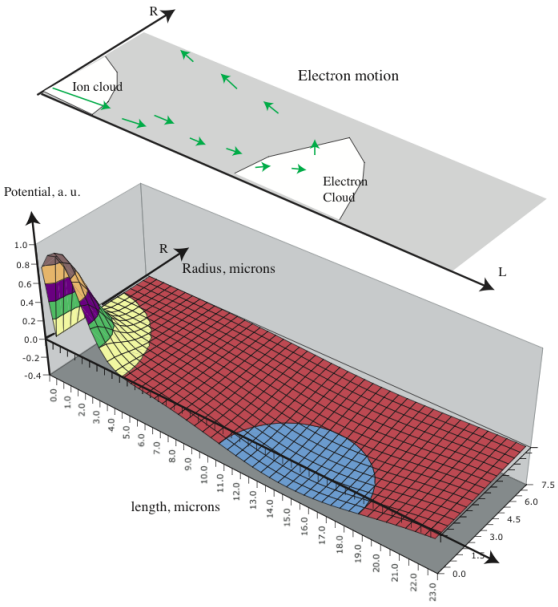

FIG. 7: Figure 7 shows the general picture of the unipolar arc, with electron motion driven by the electric fieldl. It seems consistent with the references to assume that the electron current driven by this potential could be a transient.

remains roughly constant as the arc develops. A significant component of the net surface charge is due to the field emitted currents, which are variable, even at comparatively low surface fields. As the surface electric field under the plasma rises to values on the order of a few GV/m, it becomes possible for the whole surface area under the plasma to field emit. At a field of 5 GV/m with a current density of 10^6 A/m^2, this current would amount to 6×10^{24} electrons/m^2/s, capable of shorting out the plasma charge in 1 ns. Since the field emitted currents go like $\sim E^{14}$, higher surface fields could cancel out the net plasma charge in a much shorter time, essentially turning the arc off locally. In practice, the plasma should be large enough that the arc could re-establish itself elsewhere. This mechanism could explain the "chicken-track" pattern of damage in some structures. It is also consistent with the quantization of arcs described by G. Mesyats [26], although the mechanism would be different than the Ohmic heating of liquid metal that results in "ectons".

VI. FATIGUE, CREEP, FIELD EVAPORATION, ELECTROMIGRATION AND OHMIC HEATING

There are a number of physical mechanisms that affect the surface of highly stressed structures, triggering a failure of the surface. As mentioned in Part I, the environment of the field emitter / breakdown site is very close to its ultimate electric field limits due to many effects: field evaporation, which tends to dull or smooth asperities, and a number of other effects, including fa-

tigue, creep, electromigration and Ohmic heating all of which can make asperties sharper. Since all these effects are strongly dependent on the local electric field, which is dependent on a local geometry that is also not well known, it is difficult to evaluate the relative strength these effects over the the appropriate range of surface fields. It becomes useful, however, to look at the dependence of individual mechanisms on the electric field, since the rates for these processes decrease rapidly as the field is reduced from its maximum value.

Field evaporation is discussed at length in references such as Chapter 2 of Ref. [27]. This effect is due the the electric field pulling individual atoms out of the potential well of the material. The flux produced depends strongly on the electric field, with data showing field dependencies from E^{50} to E^{150}, the high exponent leading to preferential erosion of more exposed atoms, producing a general smoothing effect. For most smooth surfaces the surface fields at which this process occurs are a few 10s of GV/m, however these surfaces are unlikely to occur naturally in real structures so the effect would likely be significant at lower fields for surfaces with some micro-roughness.

Fatigue and creep are active at the atomic level allowing strain in solid materials to respond to cyclic stress [28]. Since stress is proportional to E^2, we would expect that this mechanism might be stronger farther from the ultimate materials limit than effects with higher exponents. For creep, it is customary to consider a the "creep exponent", n_C, where

$$d\epsilon/dt = C\sigma^{n_C} e^{-E_c/kT}$$

where ϵ, σ and n_C are the strain, stress, and the creep exponent. In this case, $n \leq 10$, thus the creep rate as a function of E could proceed with an exponential dependence as large as E^{20}. Any measurements of the "creep exponent" must be done over a fairly narrow range of failure rates, and this may constrain the range of n and one would expect the this number would be a function of the stress.

Electromigration describes how high current density electron flows and high temperatures can cause surface ions and atoms to move in the direction of the electron current [29]. This phenomenon is common in integrated circuits where small gaps, high fields and currents are present. C. Antoine has pointed out to us that the environment of a breakdown site may be susceptible to this mechanism because of the high current densities moving near a field emitter, and the elevated temperature that may be expected at the breakdown site [30].

The Black equation can be used to express the failure rate, R which is given by,

$$R = BJ^n e^{-E_a/kT},$$

where E_a, J, n, B and kT are: note that for field emission near 10 GV/m, $J \sim E^{14}$, so $R \sim E^{28}$. fatigue/creep [31]

As mentioned elsewhere, Ohmic heating and thermal diffusivity, modified by the Nottingham effect (which also cools the surface) will determine the temperature of asperities exposed to high currents [32]. Experiments with exploding wires have been done for many years, demonstrating that high current densities can easily vaporize small conductors, however as the shape of the conductors departs from a cylinder, the thermal diffusivity must be considered. The volume of material that must be heated is determined by the thermal diffusivity distance

$$r = \sqrt{Dt},$$

where the thermal diffusivity constant for copper is roughly 10^{-4} m^2/s [33]. under these circumstances the volume of material in thermal equilibrium would be roughly $0.3_{[\mu m]}\sqrt{t_{[sec]}}$, generally a much larger dimension than the volume that is heated Ohmically.

VII. CONCLUSIONS

We have developed a model of arcing that attempts to identify and model, to some degree, all the processes that might contribute to rf arcing. This paper attempts to idendify and model the primary physical mechanisms by which surfaces can interact with these arc plasmas. While the list of mechanisms may be incomplete, they should serve as a useful guide or starting point for further developments or other work. We have not based our model on other work in the literature so these papers should provide a self consistent alternative to existing models, with which we generally differ.

We have consistently argued that arcing can be described as a surface fracture, followed by ionization of fracture fragments, exponential growth of the plasma density and local damage caused essentially by unipolar arcs.

VIII. ACKNOWLEDGMENTS

The work at Argonne is supported by the U.S. Department of Energy Office of High Energy Physics, by Contract No. DE-AC02-06CH11357. The work of Tech-X personnel is funded by the Department of Energy under Small Business Innovation Research Contract No. DE-FG02-07ER84833.

[1] Z. Insepov, J. Norem, D. Huang, S. Mahalingam, S. Veitzer, This journal.

[2] Z. Insepov, J. Norem and Z. Veitzer, Nucl. Instr. and

Meth. in Phys. Res. B, **B268** (2010) 642.
[3] A. Anders, S. Anders, and M. A. Gundersen, Phys. Rev. Lett. *71*, 364 (1993).
[4] A. Anders, *Cathodic Arcs: From Fractal Spots to Energetic Condensation*, Springer, New York (2008).
[5] M. Bradley, J.M.E. Harper, J. Vac. Sci. Techn. **A6** 2390 (1988) .
[6] W.L. Chan, E. Chason, J. Appl. Phys. **101**, 121301 (2007).
[7] Z. Insepov, I. Yamada, Nucl. Instr. Meth. B 148 (1999) 121
[8] R. Feynman, T. E. Leighton, and M. Sands, *Feynman Lectures on Physics, Vol II*, Addison Wesley New York (1963), Section 6-11.
[9] L. Tonks, Phys. Rev. **48** 562 (1935).
[10] Y. Frenkel, Phys. Zs. Sowjetunion, **8**. 675 (1935).
[11] J. He, N. M. Miskovsky, P. H. Cutler and M. Chung, J. Appl. Phys., **68**(4), 1475, (1990).
[12] A. L. Prergenzer J. Appl. Phys. **58**.(12), 4509 (1985).
[13] G. Arnau-Izquierdo, Private Communication (2010).
[14] R. V. Latham, ed., *High Voltage Vacuum Insulation:basic concepts and technological practice*, Academic Press, (1995).
[15] H. Padamsee, J. Knobloch, T. Hays, *RF Superconductivity for Accelerators*, Wiley-Interscience, New York (1998).
[16] W. P. Dyke and J. K. Trolan, Phys. Rev. **89** (1953) 799.
[17] F. Rohrbach, CERN Yellow Report 71-28, CERN, Geneva, SW (1971).
[18] M. Luong, H. Safa, B. Bonin, T. Junquera, A. Le Goff. and S. Maissa, J. Phys. D: Applied Physics, **30** 1248 (1997).
[19] COMSOL software, http://www.comsol.com/
[20] G. Mueller, University of Wuppertal, Private Communication (2007).
[21] D. Lysenkov and G. Mueller, Int. J. Nanotech. **2**, 239 (2005).
[22] A. E. Robson and P. C. Thonemann, *Proc. Phys. Soc*, **73** 508 (1959).
[23] F. R. Schwirzke, IEEE Trans. on Plas. Sci., **19**, 690 (1991)
[24] F. Schwirzke, X. K. Maruyama, IEEE Trans. on Plas. Sci., **21**(5) 410, (1993).
[25] Workshop on Unipolar Arcs, https://twindico.hep.anl.gov/indico/conferenceDisplay.py?confId=69, Jan, 29, 2010, Argonne National Lab, Chicago (2010).
[26] G. A. Mesyats, *Explosive Electron Emission*, URO Press, Ekaterinberg, Russia (1998).
[27] M. K. Miller, A. Cerezo, M. G. Hetherington, and G. D.W. Smith, *Atom Probe Field Ion Microscopy*, Oxford Science Publications, Oxford, (1996).
[28] N. E. Dowling, *Mechanical Behavior of Materials*, Prentice Hall, Upper Saddle River, NJ (1999).
[29] J.R. Black, Proceedings of the IEEE **57** (9)1587 (1969).
[30] C. Antoine, Private Communication, (2010)
[31] J.R. Black, IEEE Transactions on Electron Devices **16**(4): 338 (1969).
[32] W. B. Nottingham, Phys. Rev. **49**, 78 (1936).
[33] J.P. Holman, *Heat Transfer*, 9th Ed., McGraw-Hill, (2002).